



Article

# Omics Analysis Unveils the Pathway Involved in the Anthocyanin Biosynthesis in Tomato Seedling and Fruits

Rui He, Kaizhe Liu , Shuchang Zhang, Jun Ju, Youzhi Hu, Yamin Li , Xiaojuan Liu and Houcheng Liu \*

College of Horticulture, South China Agricultural University, Guangzhou 510642, China; ruihe@stu.scau.edu.cn (R.H.); 1836945107@stu.scau.edu.cn (K.L.); shuchangzhang@stu.scau.edu.cn (S.Z.); jujun-mail@stu.scau.edu.cn (J.J.); youzhihu@stu.scau.edu.cn (Y.H.); yaminli@stu.scau.edu.cn (Y.L.); liuxjy628@stu.scau.edu.cn (X.L.)

\* Correspondence: liuhch@scau.edu.cn; Tel.: +86-020-85-280

**Abstract:** The purple tomato variety ‘Indigo Rose’ (InR) is favored due to its bright appearance, abundant anthocyanins and outstanding antioxidant capacity. *SlHY5* is associated with anthocyanin biosynthesis in ‘Indigo Rose’ plants. However, residual anthocyanins still present in *Slhy5* seedlings and fruit peel indicated there was an anthocyanin induction pathway that is independent of *HY5* in plants. The molecular mechanism of anthocyanins formation in ‘Indigo Rose’ and *Slhy5* mutants is unclear. In this study, we performed omics analysis to clarify the regulatory network underlying anthocyanin biosynthesis in seedling and fruit peel of ‘Indigo Rose’ and *Slhy5* mutant. Results showed that the total amount of anthocyanins in both seedling and fruit of InR was significantly higher than those in the *Slhy5* mutant, and most genes associated with anthocyanin biosynthesis exhibited higher expression levels in InR, suggesting that *SlHY5* play pivotal roles in flavonoid biosynthesis both in tomato seedlings and fruit. Yeast two-hybrid (Y2H) results revealed that *SIBBX24* physically interacts with *SIAN2-like* and *SIAN2*, while *SIWRKY44* could interact with *SIAN11* protein. Unexpectedly, both *SIP1F1* and *SIP1F3* were found to interact with *SIBBX24*, *SIAN1* and *SIJAF13* by yeast two-hybrid assay. Suppression of *SIBBX24* by virus-induced gene silencing (VIGS) retarded the purple coloration of the fruit peel, indicating an important role of *SIBBX24* in the regulation of anthocyanin accumulation. These results deepen the understanding of purple color formation in tomato seedlings and fruits in an *HY5*-dependent or independent manner via excavating the genes involved in anthocyanin biosynthesis based on omics analysis.

**Keywords:** anthocyanin biosynthesis; purple tomato; *HY5*; *MBW*; *PIFs*



**Citation:** He, R.; Liu, K.; Zhang, S.; Ju, J.; Hu, Y.; Li, Y.; Liu, X.; Liu, H. Omics Analysis Unveils the Pathway Involved in the Anthocyanin Biosynthesis in Tomato Seedling and Fruits. *Int. J. Mol. Sci.* **2023**, *24*, 8690. <https://doi.org/10.3390/ijms24108690>

Academic Editor: Wajid Zaman

Received: 9 April 2023

Revised: 8 May 2023

Accepted: 9 May 2023

Published: 12 May 2023



**Copyright:** © 2023 by the authors. Licensee MDPI, Basel, Switzerland. This article is an open access article distributed under the terms and conditions of the Creative Commons Attribution (CC BY) license (<https://creativecommons.org/licenses/by/4.0/>).

## 1. Introduction

Anthocyanins comprise a class of primary hydrosoluble pigments belonging to flavonoids, which are widely distributed in plants and confer various colorations in fruit, flower, seed and leaf. Anthocyanins are essential antioxidants that not only play their crucial roles in protecting plants from various biotic and abiotic stressors (i.e., cold, drought, UV irradiation, pathogen) but also contribute to decreasing the risk of certain types of cardiovascular and neurodegenerative diseases and cancer in the human body [1–3]. Anthocyanin biosynthetic pathways have been intensively studied in many species, and various structural genes and transcription factors have been well characterized in a strongly conserved pathway [4–6]. The regulation of anthocyanin biosynthesis is controlled by early biosynthetic genes (i.e., phenylalanine ammonia-lyase (*PAL*), 4-coumaryl:CoA ligase (*4CL*), chalcone synthase (*CHS*), chalcone isomerase (*CHI*) and flavanone 3-hydroxylase (*F3H*)) and late biosynthetic genes (i.e., flavonoid 3′5′-hydroxylase (*F3′5′H*), dihydroflavonol 4-reductase (*DFR*), anthocyanidin synthase (*ANS*), glutathione-S-transferase (*GST*) and flavonol-3-glucosyltransferase (*3GT*)) [7]. Most genes involved in anthocyanins biosynthesis could be activated or repressed by specific transcription factors as well as controlled

by a ternary MYB–bHLH–WD repeat (MBW) transcriptional complex, which consists of basic helix–loop–helix (bHLH) R2R3–MYB transcription factors and WD40-repeat proteins [8]. In addition, other regulatory factors, such as HY5, ERFs, PIFs, BBXs, and WRKYs, also participated in the regulation of anthocyanin biosynthesis [9–12]. Previous studies have proved that *AtBBX21*, *AtBBX22* and *AtBBX23* induced the accumulation of anthocyanins in Arabidopsis [13–16], while *AtBBX24*, *AtBBX25* and *AtBBX32* inhibit anthocyanin accumulation [17–19]. *SIBBX20* directly binds the promoter of the anthocyanin biosynthesis gene *SIDFR* to enhance anthocyanin biosynthesis in tomato fruits [20]. *MdBBX22* induced *mdm-miR858* expression via bounding to its promoter, thus governing anthocyanin accumulation in apples [21]. Additionally, members of the B-box (BBX) protein family (i.e., *BBX18/20/21/23/24/33*) directly conjunct with HY5 cooperatively regulate anthocyanin synthesis in Arabidopsis [22]. Furthermore, results showed that a WRKY gene negatively regulates the complex MYB–bHLH–WD40 petunia (*Petunia hybrida*) and Arabidopsis thaliana [23]. *PpWRKY44* could significantly promote light-induced anthocyanin accumulation in red pear fruit via binding to the promoters of *PpMYB10* [24].

The tomato (*Solanum lycopersicum*) is one of the most consumed vegetable products around the world. In most of the cultivated tomatoes, anthocyanins are generally undetectable in fruit. Cultivation attempts have been made to improve the anthocyanin content in tomato fruit. ‘Indigo Rose’ (InR), a purple tomato variety that contains the Aft locus and recessive atv locus, exhibits a high-level accumulation of anthocyanin on the fruit peel in a light-dependent manner [25]. Thus, ‘Indigo Rose’ has been frequently taken to underly the molecular mechanism of anthocyanin synthesis in purple tomato fruit [26–28]. Previous studies revealed R2R3–MYB transcription factor *SIAN2-like* as an active and critical regulator of anthocyanin biosynthesis, while *SIMYBATV* was identified as the regulatory repressor via competing for the binding of *SIAN2-like* to *SIAN1* [27].

HY5 (Elongated Hypocotyl 5), as a vital regulator of light-dependent development in higher plants, exhibits a dominant function in hypocotyl elongation and lateral root development as well as pigment accumulation [29]. To date, most of the genes and transcription factors involved in anthocyanin regulation were highly associated with HY5. The HY5 protein directly binds to either G-box or ACE-box in the promoters of anthocyanin biosynthetic genes such as *CHS* and *DFR*, then activates their expression, positively regulating anthocyanin accumulation [30]. *CaHY5* can bind to the promoter of *CaF3H*, *CaF3'5'H*, *CaDFR*, *CaANS* and *CaGST*, which are well related to anthocyanin biosynthesis or transport, and thereby promote anthocyanin accumulation in pepper hypocotyl [31]. However, residual anthocyanins have still been present in *hy5* mutants of Arabidopsis, which indicates that there is an anthocyanin induction pathway that is independent of HY5 in plants [30,32]. This result has been well proved in *Slhy5* mutants of tomatoes via analyzing the transcriptome of multiple tissues, which has found eight candidate transcription factors were likely involved in anthocyanin production in tomatoes in an HY5-independent manner [11]. In the present study, we found that anthocyanins accumulated on the surface of hypocotyls in InR tomato seedlings, but not *Slhy5* seedlings, at cotyledon emergence. Unexpectedly, residual anthocyanins also accumulated both in the cotyledon and hypocotyls of *Slhy5* seedling, which displayed obvious spatiotemporal specificity. Meanwhile, the InR fruit peel accumulated large amounts of anthocyanins, particularly in the light-exposing part, while *Slhy5* contained a lower anthocyanin content on the peel of the fruit shoulder and no anthocyanins accumulated in the peel of the shading part. Therefore, whether other transcription factors substitute or compensate for HY5 to regulate the anthocyanin accumulation? Advances in transcriptomics and metabolomics play pivotal roles in uncovering complex biological mechanisms of diversified pathways in plants [33,34].

The objectives of this study were to reveal the anthocyanin variation in seedlings and fruit of tomato (‘Indigo Rose’ (InR) and *Slhy5* mutants) at different developmental stages and excavate the candidate HY5-dependent or independent transcription factors involved in anthocyanin biosynthesis in the seedling and fruit via omics analysis.

## 2. Results

### 2.1. Morphological Characterization of *InR* and *Slhy5* Seedling and Fruit

On the stage in which hypocotyl emergence and cotyledons still close, the surface of hypocotyls of *InR* seedlings exhibited purple color, whereas *Slhy5* seedlings displayed white color (hardly accumulate anthocyanins) and longer hypocotyl (Figure 1a and Figure S1). Considerable anthocyanins accumulation was observed in cotyledons and hypocotyls of *InR* seedlings once exposed to light (Figure 1a and Figure S1). However, *Slhy5* seedlings developed an opposite phenotype and displayed obvious spatiotemporal specificity in anthocyanin production. Briefly, in *Slhy5* seedlings, the anthocyanin accumulated first in the upper part of the hypocotyls and then gradually developed in the lower part in a light-dependent manner (Figure 1a and Figure S1). The anthocyanin content both in cotyledons and hypocotyls of *Slhy5* seedlings was lower than those of *InR* seedlings, respectively (Figure 1c and Figure S1).

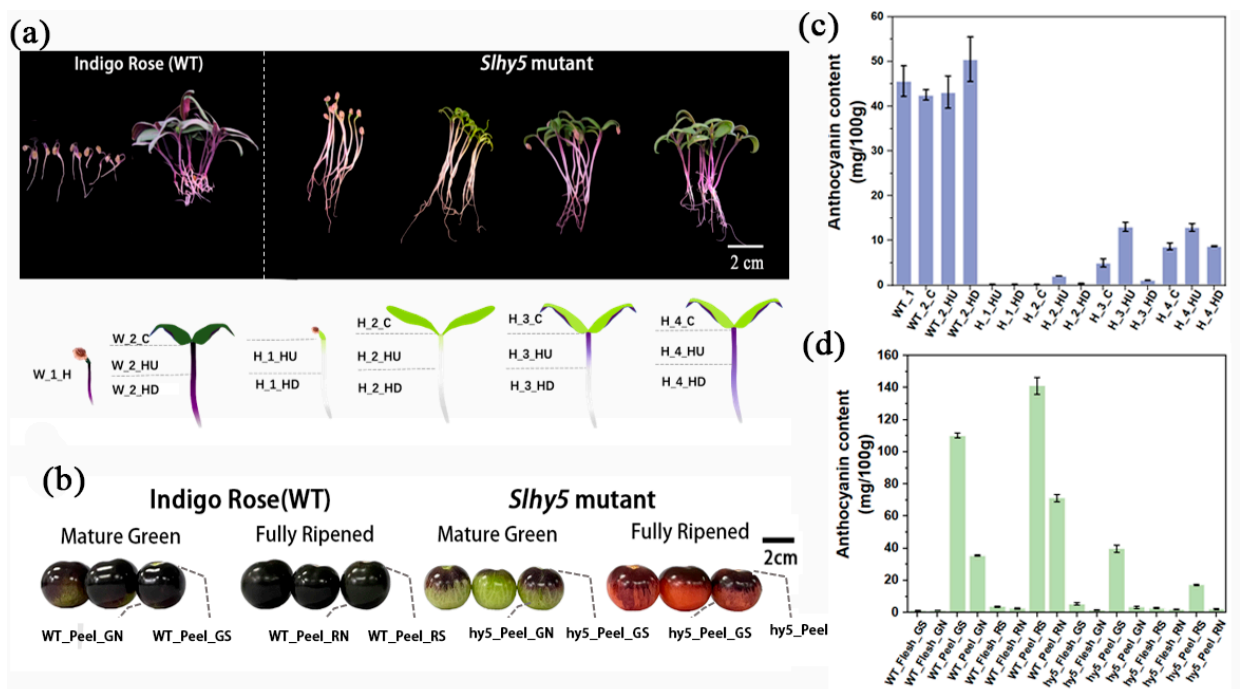


**Figure 1.** Morphological characterization of *InR* and *Slhy5* seedling and fruit. (a) Photograph showing the seedling phenotypes of different stages of *InR* and *Slhy5* seedlings for 4–7 days. (b) The phenotype of fruit from *InR* and *Slhy5* mutants at the mature green-mature stage and fully mature stage. (c) The anthocyanin content of *InR* and *Slhy5* seedling in different tissues. (d) The anthocyanin content of *InR* and *Slhy5* fruits at the green-mature stage and fully ripened stage both in peel and flesh. Error bars indicate SD ( $n > 3$ ).

Anthocyanin content just accumulated in peels at the green-mature stage and fully mature stage in *InR* and *Slhy5* fruits, and few anthocyanins were found in the fruit flesh (Figure 1b,d and Figure S2). Additionally, higher anthocyanins accumulated in the light-exposing peel part of *InR* fruits than in the shading part (Figure 1b,d). Unexpectedly, residual anthocyanins have still been present in the peel of the *Slhy5* fruit shoulder, though the anthocyanins contents were lower than the *InR* fruit peel. However, anthocyanin accumulation was hardly detected in the shading peel part of the *Slhy5* fruit (Figure 1b,d). These observations suggested that *Slhy5* had a predominant role in tomato pigmentation in a light-dependent manner, and there might be some regulators controlling anthocyanin biosynthesis in an *HY5*-independent manner.

## 2.2. Changes of Metabolites and Genes Expression in the Cotyledon of InR Seedlings and *Sllhy5* Seedlings

The color of cotyledon and hypocotyl was transformed continuously from green to purple during seedling development in InR seedlings and *Sllhy5* seedlings. To explore the changes of metabolites and gene expression during InR and *Sllhy5* seedling development, metabolic and transcriptome analysis of cotyledon, the upper and lower part of the hypocotyl were carried out at different developmental stages, respectively (Figure 1a). PCA was performed on detected metabolites to demonstrate the similarity in metabolic profiles among the samples (Figure S3). In the two-dimensional PCA plot, three biological replicates of each sample tended to group, indicating the high reproducibility of the generated metabolome data (Figure S3). Many metabolites and genes in the seedling varied considerably in terms of different tissues of different varieties. Therefore, variation of metabolites and gene expression in three parts (cotyledon, upper and lower part of the hypocotyl) of InR seedlings and *Sllhy5* seedlings was investigated, respectively.

Four metabolite groups were observed in cotyledon based on the level of annotation of metabolite similarity. Group 1, which metabolites levels of InR seedlings cotyledon (W\_2\_C) were obviously higher than those in *Sllhy5* seedlings (H\_2\_C, H\_3\_C and H\_4\_C), including tulipanin, rutin, butin etc., belonged to flavonoids, flavones and flavonols, anthocyanins according to KEGG analyses (Figure S4). So, anthocyanins and flavonoids might be responsible for the distinction of purple coloration of cotyledon between InR and *Sllhy5* seedlings.

The transcriptome data validated the authenticity and accuracy of the metabolic analysis. A weighted gene co-expression network analysis (WGCNA) was performed on the genes of cotyledon. A slight relationship with purple coloration was displayed in the green module (Figure 2b), and the genes related to this module were annotated according to KEGG pathway enrichment analysis, which involved the flavonoid biosynthesis pathways (Figure 2c). Anthocyanins metabolism-related transcriptional factors (i.e., *SIAN1*, *SIAN2*, *SIAN2-like*) and the structural genes (i.e., *SIPAL*, *SI4CL*, *SICHS*, *SICHI*, *SIDFR*, *SIANS*) displayed higher expression levels in the cotyledon of InR seedlings than *Sllhy5* seedlings (Figure 2c,d). Meanwhile, the expression of these genes increased with the development of *Sllhy5* seedlings cotyledon, which is consistent with the increasing trend of flavonoid and anthocyanins contents (Figure 2c,d).

## 2.3. Changes of Metabolites and Genes Expression in the Upper Part of the Hypocotyl of InR Seedlings and *Sllhy5* Seedlings

In the upper part of hypocotyl, the differential metabolites in group 1, which was positively correlated and had similar consistent patterns with the purple coloration in the hypocotyl, also contained a variety of flavonoids such as petunidin 3-O-glucoside, tulipanin, isotrifoliin (Figure 3a). The KEGG enrichment analysis displayed that the terms 'Flavone and flavonol biosynthesis', 'Photosynthesis', 'Anthocyanin biosynthesis', 'Vitamin B6 metabolism', and 'Starch and sucrose metabolism' were significantly enriched in the Group 1 (Figure S5). WGCNA identified genes in the black module with significant co-expression with the biosynthesis of the metabolite in the flavonoid pathway, which was responsible for the purple coloration observed in the upper part of the hypocotyl (Figure 3b).

KEGG enrichment analysis was performed on the genes in the black module and showed that these DEGs were enriched mainly in flavonoid biosynthesis pathways (Figure 3c). Consistent with the data from the transcriptomic analysis, both the anthocyanin positive regulatory genes, such as *SIAN2*, *SIAN2-like*, *SIAN1I* and *SIAN11* (except for the negative regulatory genes *SIMYB7*, *SIMYB3* and *SIMYB32*) and the anthocyanin biosynthetic genes, including *SIPAL*, *SI4CL*, *SICHS*, *SICHI*, *SIF3H*, *SIF3'H*, *SIDFR*, *SIANS* and *SI3GT* (Figure 3d,e), exhibited much higher expression in the upper part of InR seedlings hypocotyl than those of *Sllhy5* seedlings. Compared with H\_1\_HU and H\_2\_HU, the genes involved in anthocyanins under H\_4\_HU and H\_3\_HU displayed higher expression levels (Figure 3d,e).

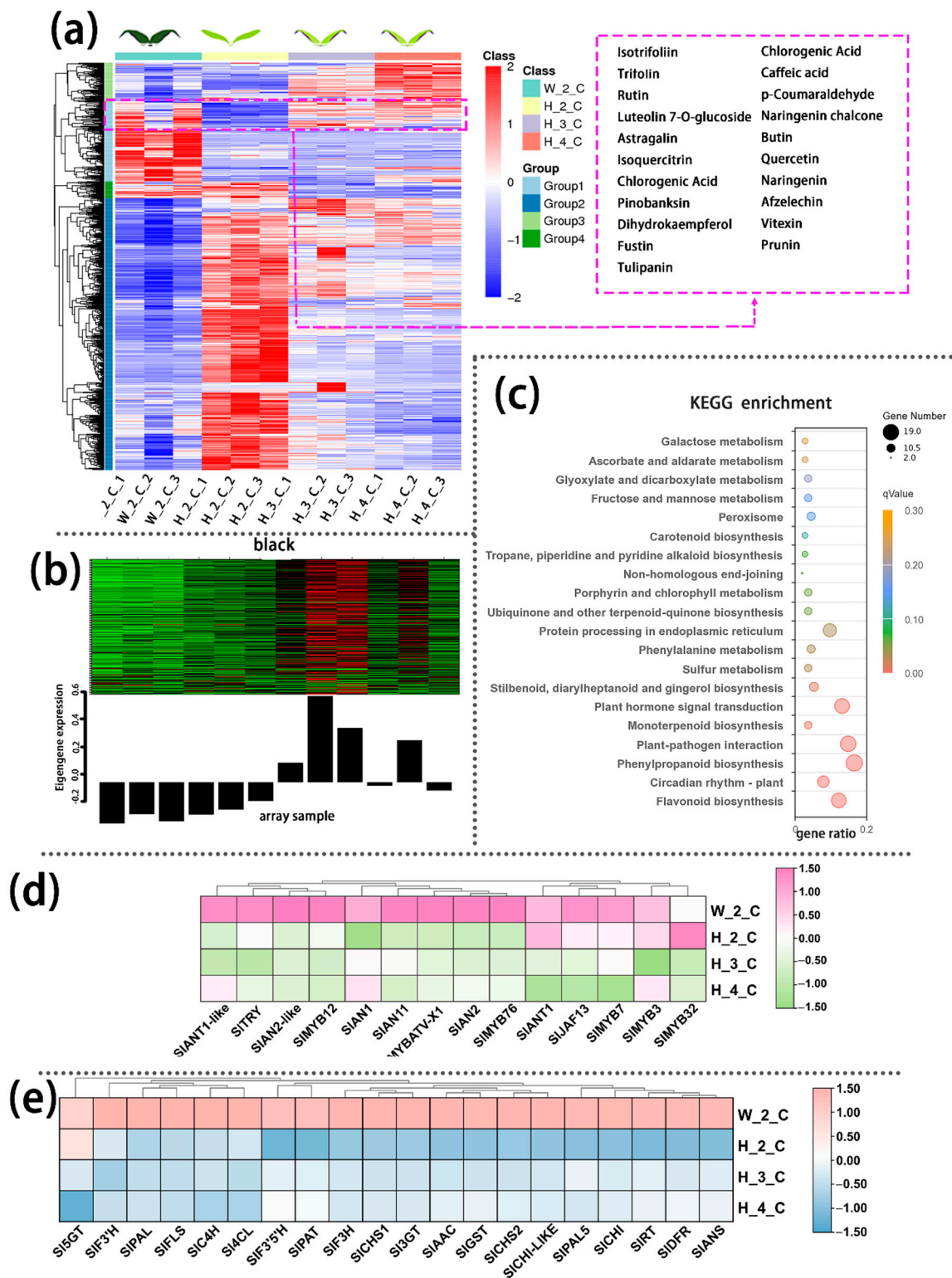


**Figure 2.** Differentially accumulated metabolites (DAMs) accumulation pattern consisted of the color variations during seedling development of cotyledon (a). The genes in the green module consisted of color variations during the seedling development of cotyledon (b). Top 20 enriched KEGG pathway enrichment of the genes in green module (c). The FKPM values of the transcriptional factors (d) and the structural genes (e) related to flavonoid and anthocyanin biosynthesis.

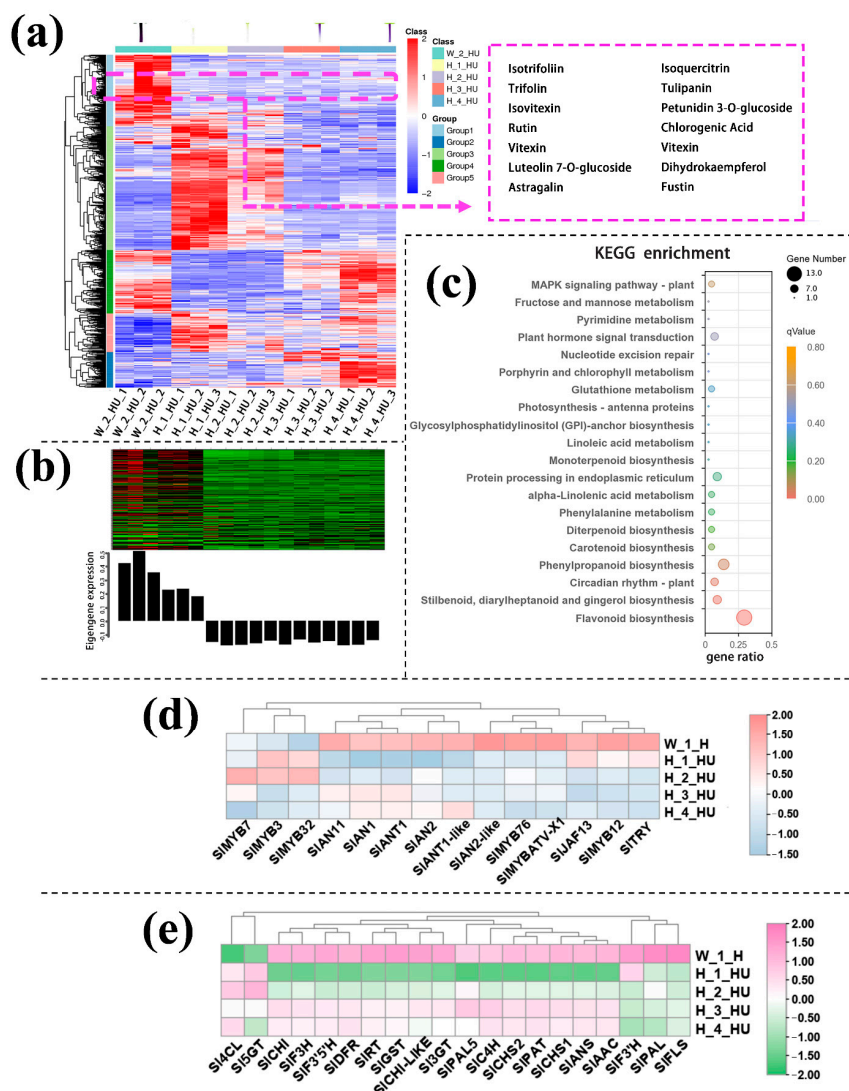


**Figure 3.** Differentially accumulated metabolites (DAMs) accumulation patterns consisted of color variations during seedling development of the upper part of the hypocotyl (a). The genes in the green module consisted of color variations during seedling development of the upper part of the hypocotyl (b). Top 20 enriched KEGG pathway enrichment of the genes in black module (c). The FKPM values of the transcriptional factors (d) and the structural genes (e) related to flavonoid and anthocyanin biosynthesis.

#### 2.4. Changes of Metabolites and Genes Expression in the Lower Part of the Hypocotyl of InR Seedlings and *Slyh5* Seedlings

Similarly, annotated metabolites in the lower part of the hypocotyl could be divided into several large groups based on similar variation tendencies, respectively. Among these metabolites, group 1 metabolites were present in higher levels in InR seedlings than in *Slyh5* seedlings, which were consistent with the color variations during seedling development. These metabolites include petunidin 3-O-glucoside, tulipanin and isotrifoliin (Figure 4a). KEGG analysis showed that these metabolites in different parts of the seedling were mainly enriched in flavone and flavonol biosynthesis and anthocyanin biosynthesis (Figure S6). The genes in mode marked by pale turquoise color according to WGCNA analysis of transcriptomic data from the lower part of the hypocotyl were consistent with the increasing trend of anthocyanin contents (Figure 4b). The KEGG enrichment analysis showed that the term ‘flavonoid biosynthesis’ pathway was significantly more pronounced (Figure 4c). Meanwhile, the expression levels of anthocyanin biosynthesis genes in the lower

part of InR hypocotyl were higher than *Slhy5* (Figure 4d,e). In addition, the expression of most anthocyanin biosynthetic genes in the lower part of the *Slhy5* seedling hypocotyl under different stages exhibited the following trend: H\_4\_HD  $\approx$  H\_3\_HD > H\_2\_HD > H\_1\_HD.

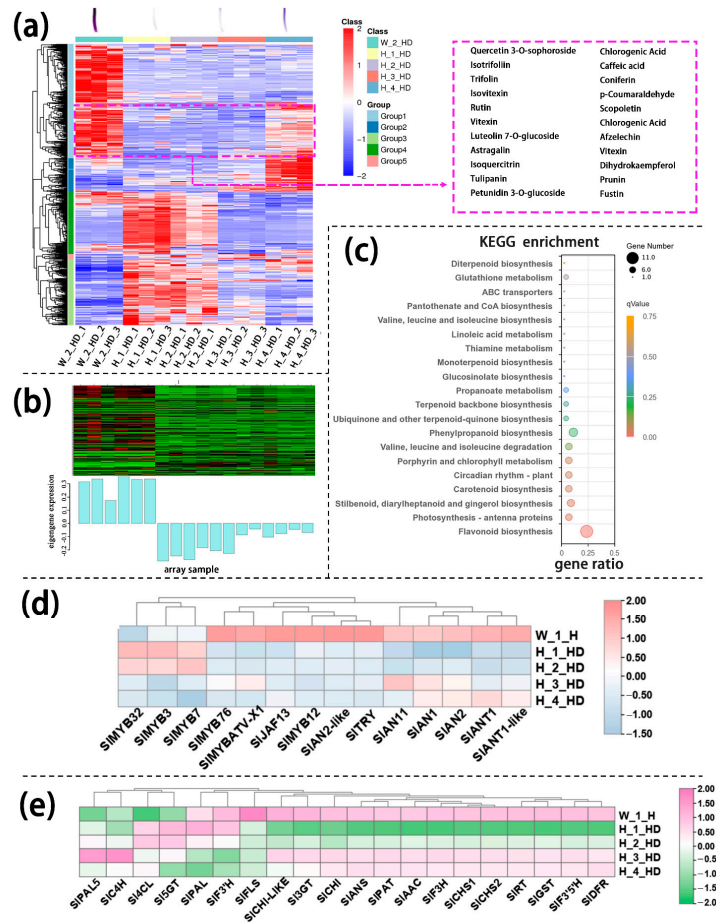


**Figure 4.** Differentially accumulated metabolites (DAMs) accumulation patterns consisted of color variations during seedling development of the lower part of the hypocotyl (a). The genes in the green module consisted of color variations during seedling development of the lower part of the hypocotyl (b). Top 20 enriched KEGG pathway enrichment of the genes in the pale turquoise module (c). The FKPM values of the transcriptional factors (d) and the structural genes (e) related to flavonoid and anthocyanin biosynthesis.

### 2.5. Changes of Metabolites and Genes Expression in Different Parts of *Slhy5* Seedling

Based on WGCNA analysis, we identified a module (marked in cyan) whose gene expression pattern was associated with the phenotype of anthocyanin synthesis in *Slhy5* seedlings at the third and fourth development stages (Figure 5a,b). Twenty-one co-expressed genes in the cyan module were significantly correlated with pigment accumulation in *Slhy5* seedlings. These indicated that bHLH (*SIAN1*) was a hub gene involved in the positive regulation of flavonoid metabolism in *Slhy5* seedlings (Figure 5c), possibly by affecting structural node genes, such as *SICHI*, *SICH5*, *SIAN3*, *SIDFR* and *SIRT*, etc.

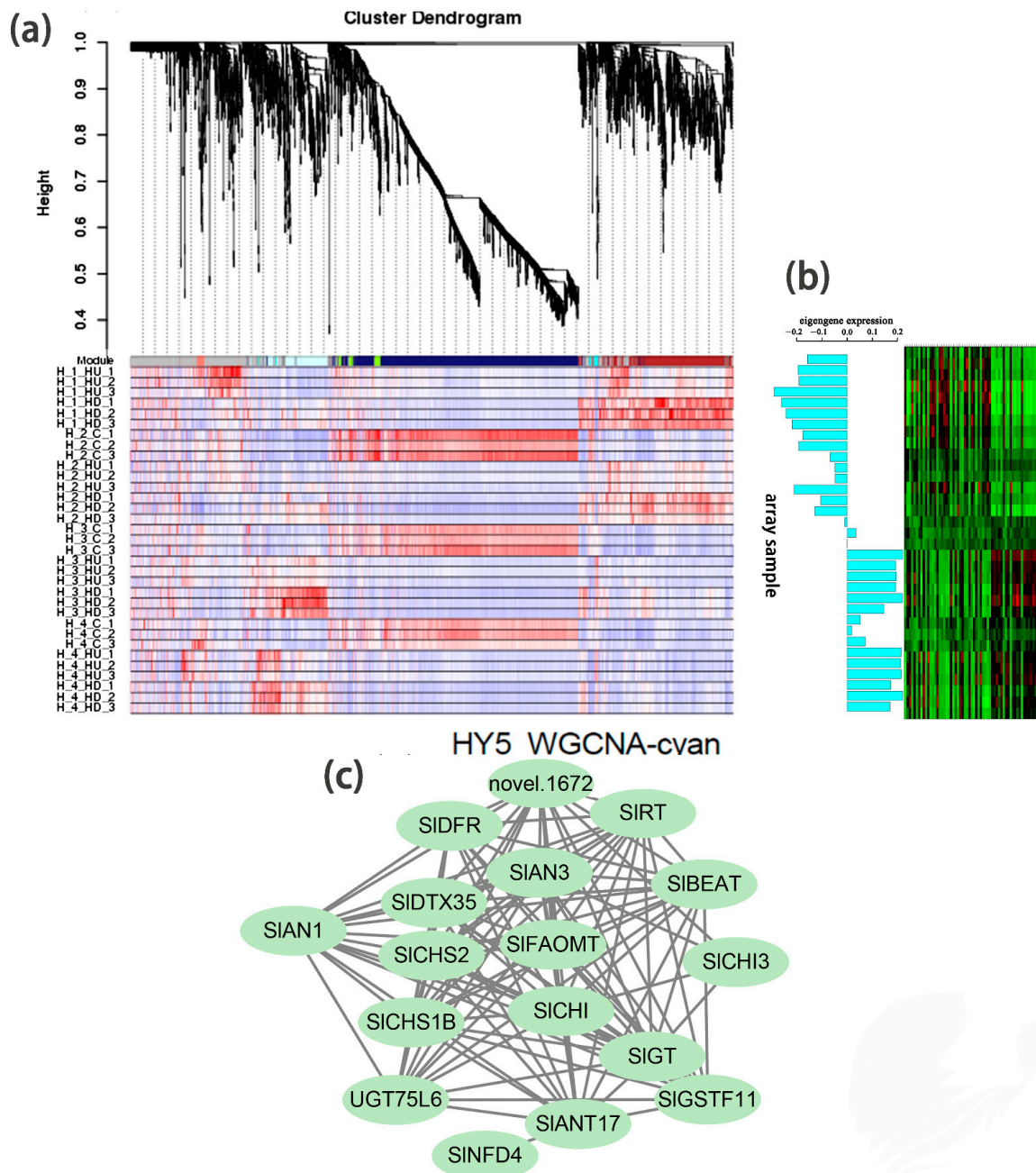


**Figure 5.** Hierarchical cluster tree showing seven modules obtained by WGCNA in *Slhy5* seedlings (a). Differential expression of genes in the accumulation pattern consisted of color variations during seedling development of *Slhy5* seedlings (b). Interaction network of DEG in the cyan model in *Slhy5* seedling (c).

## 2.6. Screening of Differentially Expressed Genes of Tomato Fruit

Similar to seedlings, residual anthocyanin production was also observed in the peel of the *Slhy5* fruit shoulder, whereas anthocyanin was almost undetectable in the shading part of the *Slhy5* fruit (Figure 1b,d). To underly gene expression changes over the fruit peel of InR and *Slhy5*, RNA-Seq analysis was conducted. The number of differentially expressed genes had a very high variance among InR and *Slhy5* fruit peel. Regarding WT-S-vs-slhy5-S (purple-colored peel of InR fruit compared to purple-colored peel of *Slhy5* fruit), a total of 2995 DEGs, including 1360 up- and 1635 down-regulated genes were detected (Figure S7). These genes were enriched in KEGG pathways related to photosynthesis, carbon fixation in photosynthetic organisms, phenylpropanoid biosynthesis, phenylalanine metabolism,



was leading to the purple peel coloration in *Sllhy5* fruit peel, that was proved that other genes or TFs were involved in anthocyanin biosynthesis in an HY5-independent manner.

To further verify expression patterns of the DEGs in seedlings and fruit, the genes *SIAN1*, *SIPAL*, *SICHS*, *SICHI*, *SIF3H*, *SIDFR*, *SIANS*, *SI3-GT*, *SIAAC* and *SIGST* were used for qRT-PCR verification (Figure S8). The qRT-PCR results were consistent with the transcriptomic analysis results.

### 2.7. The Genes Involved in the MYB-bHLH-WD40 (MBW) Complex That Activates Anthocyanidins in Tomato Fruit

To explore the regulation of flavonoid metabolism, the possible interaction of flavonoid metabolism-related genes was tested utilizing yeast two-hybrid (Y2H) assays. *SIPIF1*, *SIPIF3*, *SIAN2-like*, *SIAN2*, *SIAN11*, *SIAN1*, *SIHY5*, *SIJAF13*, *SIBBX24* and *SIWRKY44* were selected for the candidate genes based on the RNA Sequencing results, which might contribute to anthocyanin biosynthesis. We found that *SIBBX24* physically interacts with *SIAN2-Like* and *SIAN2* but not with *SIAN11* in yeast, while *SIWRKY44* could interact with *SIAN11* protein only and showed no affinity for other genes. Additionally, these results indicated that *SIBBX24* could interact with *SIPIF1* and *SIPIF3* but not *SIPIF4*. Unexpectedly, *SIAN1* and *SIJAF13* displayed the same physical interaction, which could interact with both *SIPIF1* and *SIPIF3* (Figure 7).

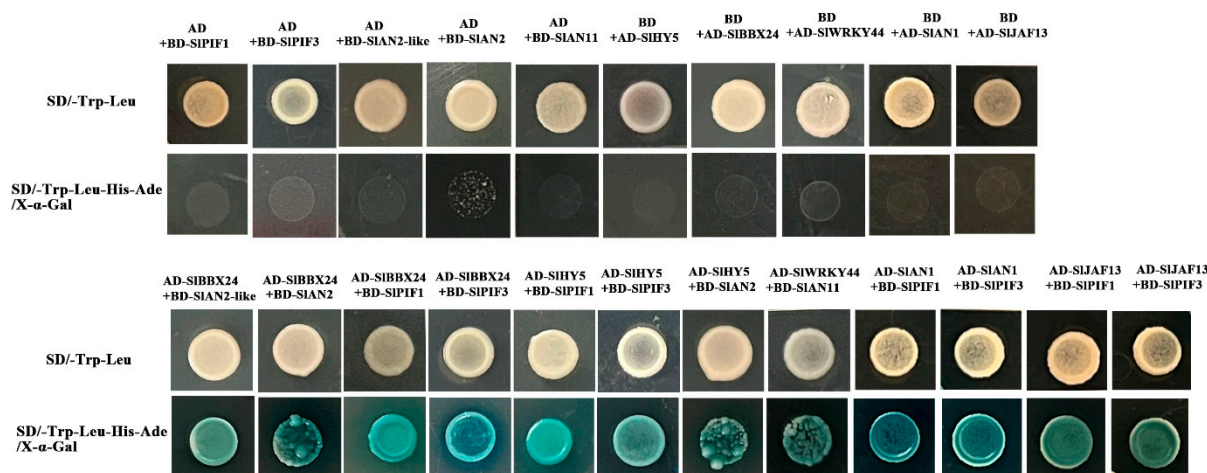


**Figure 7.** Yeast two-hybrid assay of the protein interactions between candidate genes involved in the components of the MBW complex that activates anthocyanidins in tomato.

### 2.8. *SIBBX24* Physically Interacts with Regulators of Light Signaling and Anthocyanin Biosynthesis

To further explore whether *SIBBX24* physically interacts with regulators of light signaling and anthocyanin biosynthesis, we conducted bimolecular luciferase complementation imaging (LCI) assays in *Nicotiana benthamiana* leaves. Luminescence was observed in leaves that co-expressed *SIBBX20-nLUC* and *cLUC-SIHY5*, *cLUC-SIPIF1*, *cLUC-SIPIF3*, *cLUC-SIAN2-like*, *cLUC-SIAN2*, *cLUC-SIAN11*. LUC signals were not detectable in the three controls. These results suggest that *SIBBX24* associates with the transcription factors involved in the light-signaling pathway (*SIHY5*, *SIPIF1*, *SIPIF3*) and anthocyanin biosynthesis (*SIAN2-like*, *SIAN2*, *SIAN11*) in living plant cells (Figure 8).

### 2.9. *SIBBX24* May Be Involved in Anthocyanin Accumulation in Tomato Fruit Peels

To investigate whether the biosynthesis of anthocyanin is regulated by candidate genes, a target gene of *SIBBX24* was silenced by the VIGS approach. Compared to the empty vector control, the expression of *SIBBX24* was reduced at 7 days after infiltration, and anthocyanin was less vibrant than that of control fruits (Figure 9). qRT-PCR analyses were performed to test the expression changes of the genes involved in anthocyanin biosynthesis. As shown in Figure 8, silencing of *SIBBX24* inhibited the expression levels of

anthocyanin structural genes, including EBGs (*SIC4L* and *SICH51*) and LBGs (*SIDFR* and *SIANS*) as well as the positive regulators (*SIAN1*, *SIAN2*, *SIAN2-like*, *SIAN11*, *SIHY5*), and increased the expression levels of negative regulators (*SIMYBATV*, *SITRY* and *SIMYB76*) (Figure 9). Therefore, it suggests that *SIBBX24* might be one of the important regulators in the regulatory chain of anthocyanin biosynthesis in tomato fruit.

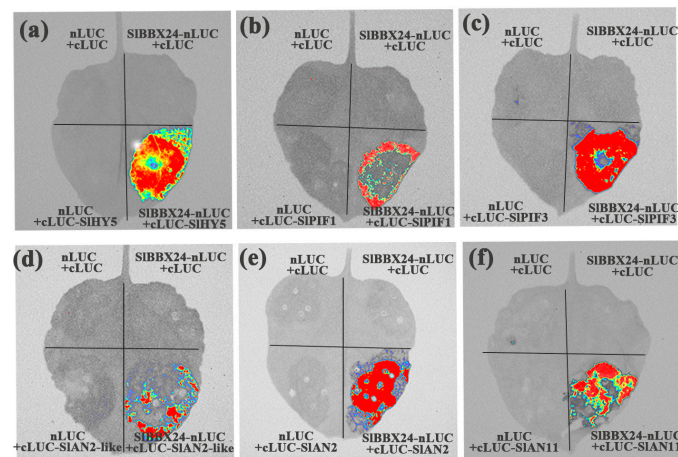


**Figure 8.** Interactions between *SIBBX20* and *SIHY5* (a), *SIPIF1* (b), *SIPIF3* (c), *SIAN2-like* (d), *SIAN2* (e), *SIAN11* (f) in firefly luciferase complementation imaging (LCI) assays in planta.

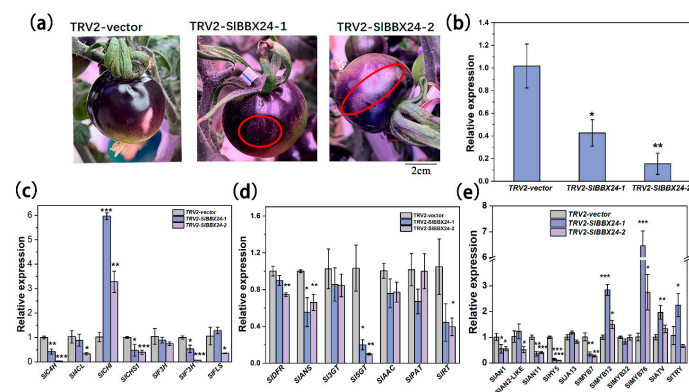


**Figure 9.** Analysis of VIGS of the *SIBBX24* gene. (a) Suppression of *SIBBX24* by virus-induced gene silencing (VIGS) retarded the purple coloration of the tomato fruit peel. (b) Relative expression of *SIBBX24* in fruit peels of TRV2-inoculated and TRV2-SIBBX24-inoculated for 7 days. (c–e) Relative expression of anthocyanin structural genes of fruit peels of TRV2-inoculated and TRV2-SIBBX24-inoculated for 7 days. Statistically significant differences between the purple zone and the green zone were determined by Student's *t*-test. (\*\*\*)  $p < 0.001$ , (\*\*)  $p < 0.01$ , (\*)  $p < 0.05$ .

### 3. Discussion

#### 3.1. Flavonoids Might Be Attributed to Major Color Differences among *InR* and *Slhy5* Mutant Seedlings and Fruit Peel

In recent years, integrated metabolomic and transcriptomic analyses as efficient tools to underly the molecular mechanisms of key metabolic pathways in plants [35–38]. A detailed description of secondary metabolic changes occurring in the whole germinated seeds as well as cotyledons, hypocotyls and roots from 3 to 9 days old tomato seedlings via LCMS profiling, which provided a new perspective to study metabolic networks controlling flavonoid biosynthesis in tomato [39]. The metabolite variants across 20 major tomato growth tissues and stages were explored by combining transcriptome and metabolome approaches, which verified novel transcription factors that control steroidal glycoalkaloids

and flavonoid pathways [40]. In the present study, an integrated analysis of the transcriptome and metabolome was conducted to reveal the differences between wild-type (InR) and *Slhy5* seedlings at different growth and development stages. A total of 987 metabolic components were accumulated specifically in InR and *Slhy5* seedlings, of which amino acids and organic acids, flavanones, flavones and isoflavonoids accounted for a large proportion (Table S2). Flavonoids, a product of the phenylpropanoid metabolism pathway, are extensively distributed in numerous plants and are composed of various subclasses, including flavanones, flavones, isoflavonoids, anthocyanins and flavonols. Anthocyanins, as a key flavonoid subgroup, are responsible for pigmentation in flowers, fruit, seed, and leaf [4]. Our metabolic profiling found metabolites in different parts of the seedling was mainly enriched in flavone and flavonol biosynthesis (Figure 2). Meanwhile, levels of flavonoids, including anthocyanins, in InR seedlings were obviously higher than those of *Slhy5* (Table S2). A KEGG analysis in WT-S-vs-Slhy5-S, Slhy5-S-vs-Slhy5-N were related to phenylpropanoid biosynthesis, phenylalanine metabolism, flavonoid biosynthesis and flavone and flavonol biosynthesis (Figure 5a). These genes were enriched in KEGG pathways related to photosynthesis, carbon fixation in photosynthetic organisms, phenylpropanoid biosynthesis, phenylalanine metabolism, flavonoid biosynthesis and flavone and flavonol biosynthesis (Figure 5a), and the gene FKPM values in InR fruit peel was higher than those of *Slhy5*. These results were well indicated that the main pigment components in InR and *Slhy5* seedlings and fruit peel were flavonoids.

### 3.2. *SlHY5* Acts as a Master Regulator to Control Anthocyanin Biosynthetic in Seedlings and Fruit of Tomato

Anthocyanin biosynthetic genes are regulated directly by the MBW complex consisting of MYB, bHLH and WDR proteins. Aft and Atv are two important loci that are well-associated with anthocyanin biosynthesis in tomatoes. MYB TFs occupy the major determinant position in the control network of anthocyanin biosynthesis and have been well demonstrated [41,42]. Four R2R3 MYB TF genes (*SIAN2*, *SIANT1*, *SIANT1-like* and *SIAN2-like*) were previously identified to regulate anthocyanin biosynthesis in tomatoes [43–45]. Two bHLH TFs, *SIAN1* and *SlJAF13*, were recently reported to regulate anthocyanin production [46]. Otherwise, a tomato WDR protein, *SIAN11*, was also involved in anthocyanin synthesis [47].

HY5 was well characterized as a positive regulator of anthocyanin synthesis in a light-dependent manner. Knock-down *SlHY5* transcription significantly reduced the anthocyanin levels both in seedlings and fruit of tomatoes [11]. *HY5* is involved in the regulation of anthocyanin biosynthesis by directly binding to MYB transcription factors, such as the production of flavonol glycosides (*MYB12/PFG1* and *MYB111/PFG3*), production of anthocyanin pigment1 (*MYB75/PAP1*) and MYB-like Domain (*MYBD*) [48]. *HY5* activates the expression of *PAP1* expression via direct binding to G-and ACE-boxes in the promoter region, positively inducing the accumulation of anthocyanin in Arabidopsis [22]. Consistently, *PyHY5* alone or interacted with *PyBBX18* activates the expression of *PyMYB10* and *PyWD40*, which subsequently regulate the anthocyanins accumulation in red pear [49]. In this study, expression levels of *SIAN2-like*, *SIAN2*, *SIAN1* and *SIAN11* were higher in InR than *Slhy5* both in seedlings and fruit, and the expression pattern of these genes was consistent with pigment accumulation (Figures 2–4 and 6). Two-hybrid (Y2H) assays determined *SlHY5* regulated anthocyanin biosynthesis through interaction with *SIAN2* (Figure 7), consistent with the result that *SlHY5* is a positive regulator of anthocyanin biosynthesis in vegetative tissues of tomato [50]. Therefore, *SlHY5* might be the master regulator to control anthocyanin accumulation in InR seedlings and fruit via mediating the transcriptional activity of an MBW complex and the enhanced expression of key genes, such as *SICHI*, *SICHS*, *SIF3H*, *SIDFR* and *SIANS*.

### 3.3. Possible Regulatory Mechanisms of Anthocyanin Biosynthesis in an *HY5*-Independent Manner in Tomato

Besides MYB and bHLH, other TF families also regulate anthocyanin biosynthesis. *SIBBX20* could directly bind to the promoter of *SIDFR* to activate its expression, thus pro-

moting anthocyanin accumulation in tomatoes [20]. In apple, *MdBBX37* interacted with *MdMYB1* and *MdMYB9*, two key positive regulators of anthocyanin biosynthesis, and inhibited the binding of those two proteins to their target genes and, therefore, negatively regulated anthocyanin biosynthesis [10]. *PpBBX18* and *PpBBX21* antagonistically regulate anthocyanin biosynthesis via competitive association with *PpHY5* in the peel of pear fruit. Also, discoveries have emphasized the importance of WRKY protein in the control of the flavonoid pathway and its relationship to the MBW complex [9]. *PpWRKY11* was able to bind to W-box cis-elements in the promoters of *PpMYB10*, then regulated anthocyanin synthesis in pear flesh [23]. In the present study, different from InR seedlings, some TFs were detected in *Slhy5* seedlings by RNA-Seq, such as WRKYs, BBXs and NACs, which might compensate for the function of HY5 and contribute to the expression of related genes involved in anthocyanin synthesis. Y2H assays revealed that *SIBBX24* could interact with *SIAN2-like* and *SIAN2*, which likely had a positive function in the regulation of anthocyanin biosynthesis (Figures 7 and 8). In addition, *SIWRKY44* also could interact with the *SIAN11* protein (Figure 7), which was consistent with the result that the WRKY factor physically interacted with the AN11 in yeast two-hybrid analysis [51]. Silencing of *SIBBX24* via virus-induced gene silencing (VIGS) led to the downregulation of the expression of structural genes and caused a decrease in anthocyanin accumulation (Figure 9). Additionally, PIFs play a role in the biosynthesis of plant pigments. *PIF3* could specifically bind to the G-box element of anthocyanin biosynthesis-related structural genes promoter to up-regulate anthocyanin accumulation in an HY5-dependent manner under far-red light [30]. Furthermore, *PIF4* negatively regulated anthocyanin accumulation by inhibiting *PAP1* transcription in Arabidopsis seedlings [52]. In this study, *SIPIF1* and *SIPIF3* could physically interact with *SIAN1* and *SIJAF13*, as well as *SIBBX24*. We speculated that *SIPIF1*, *SIPIF3*, *SIBBX24* and *SIWRKY44* might be involved in anthocyanin biosynthesis in a manner independent or dependent on *SIHY5*.

Taken together, given the PIFs and MBW were the key regulators of anthocyanin biosynthesis, we proposed a model to clearly illustrate this mechanism (Figure 10). In InR, *SIHY5* expression was induced by light and then activated the activity of the MBW complex to regulate the anthocyanin accumulation. While in *Slhy5* seedlings and fruit, PIFs or several other transcription factors might be involved in coordinating anthocyanin biosynthesis, such as BBXs and WRKYs. More thorough and rigorous molecular studies should be performed to explore the relationship of PIFs or other transcription factors which might be involved in anthocyanin biosynthesis.

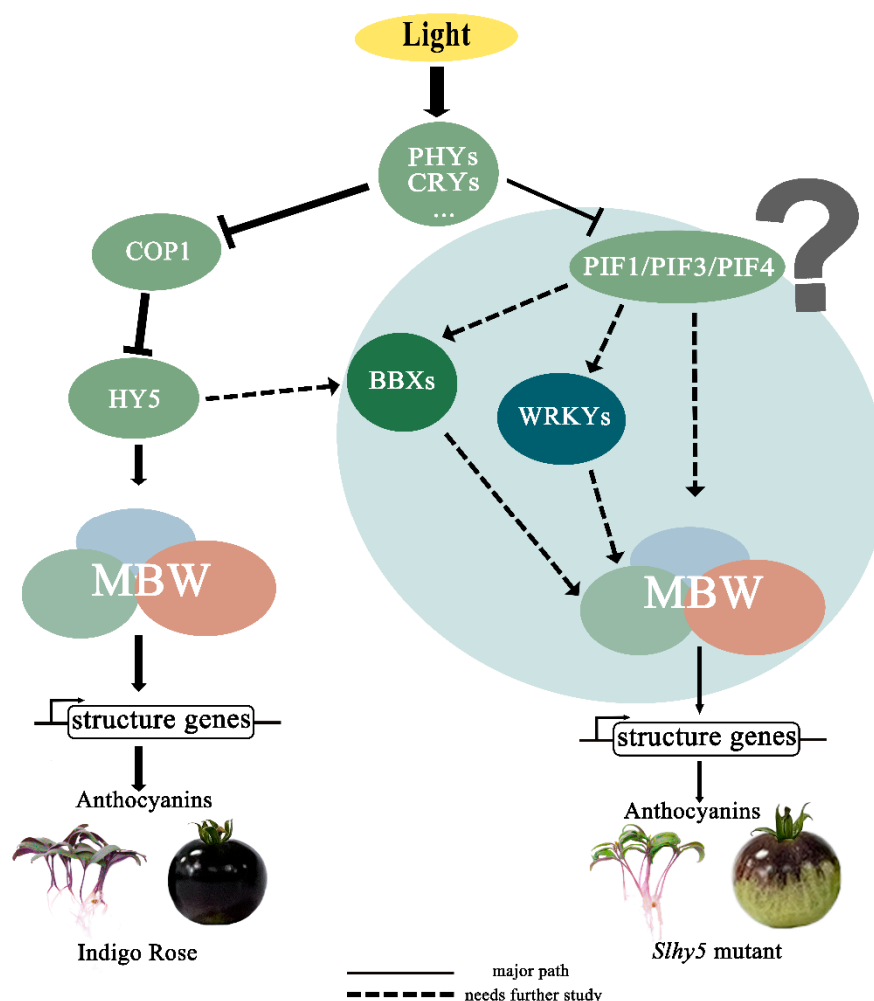


**Figure 10.** A putative model showing the anthocyanin induction pathways that might be dependent or independent of HY5 in tomatoes.

#### 4. Materials and Methods

##### 4.1. Plant Materials and Growth Conditions

The experiment was carried out in an artificial light plant factory at South China Agricultural University. The tomato seeds of wild-type (cv. 'Indigo Rose' (InR)) and *Slhy5* mutant were generously provided by Dr. Qiu of the College of Horticulture of South China Agriculture University [11]. Seeds were sanitized in 0.5% sodium hypochlorite for 15 min, then rinsed with distilled water. After being soaked in distilled water for 5 h at 25 °C, seeds were sowed in sponge cubes (2 cm × 2 cm × 2 cm) with distilled water in the plant growth chamber in the dark at 25 °C for 3 days. Then, the seedlings were grown under 300  $\mu\text{mol m}^{-2} \text{s}^{-1}$  white LEDs (Chenghui Equipment Co., Ltd., Guangzhou, China; 150 cm × 30 cm), 10/14 h light/dark photoperiod,  $24 \pm 2$  °C, and 65–75% relative humidity. The seedlings grown for the 4th, 5th, 6th and 7th days were sampled and divided into three parts: cotyledon (except for the samples on the 4th day, which cotyledons still closed), upper 1 cm of the hypocotyl, and bottom 1 cm of the hypocotyl (Figure 1a). Three biological replicates were collected for analyses, with each replicate composed of 60 seedlings. Fruits from the *Slhy5* mutants and 'Indigo Rose' were sampled at the green-mature stage and fully mature stage with three biological replicates (each replicate consisted of six fruits from different plants). The fruit peel and flesh were carefully split with a scalpel blade. The above-mentioned samples were immediately frozen in liquid nitrogen and stored at  $-80$  °C for further analysis.

#### 4.2. Anthocyanin Assay

The anthocyanin content was performed as described in a previous study with some modifications [53]. Samples (100 mg) were extracted with 1 mL buffers of pH 1.0 (50 mmol KCl and 150 mmol HCl) and pH 4.5 (400 mmol sodium acetate and 240 mmol HCl), respectively, and incubated overnight at 25 °C. The absorbance of the extract liquor was determined at 510 nm using a UV-spectrophotometer (UV-1600, Shimadzu, Kyoto, Japan).

#### 4.3. RNA Sequencing and Data Analyses

Total RNA was extracted from different parts of the seedling (Figure 1a) and the peel of fruit (Figure 1b) using the RNeasy Plant Mini kit (Qiagen, Hilden, Germany). Total amounts and integrity of RNA were assessed using the RNANano 6000 Assay Kit of the Bioanalyzer 2100 system (Agilent Technologies, Santa Clara, CA, USA). Three independent biological replicates were performed. The RNA-seq sequencing and assembly of seedling and fruit peel were performed by NovoGene Science and Technology Corporation (Beijing, China) and Genedenovo Biotechnology Co., Ltd. (Guangzhou, China), respectively. A total of 3 µg RNA was prepared for sequencing libraries using the NEB-Next Ultra™ RNA Library Prep Kit for Illumina (NEB, Beverly, MA, USA) according to the manufacturer's instructions and sequences attributed to each sample by adding index codes. The library preparations were sequenced on an Illumina HiSeq 4000 platform to generate paired-end reads. The raw sequence reads were filtered by removing adaptor sequences and low-quality sequences, and raw sequences were changed into clean reads. Then the clean reads were then mapped to the tomato reference genome sequence (ITAG 4.0) ([https://solgenomics.net/organism/Solanum\\_lycopersicum/genome/](https://solgenomics.net/organism/Solanum_lycopersicum/genome/), accessed on 18 November 2021).  $\text{Padj} \leq 0.05$  and  $|\log_2(\text{foldchange})| \geq 1$  were set as the threshold for significantly differential expression. WGCNA analyses were constructed in the BioMarker cloud platform (<http://www.biocloud.net>, accessed on 10 March 2022).

#### 4.4. Metabolite Extraction

Samples of different parts of seedling preparation, extract analysis, metabolite identification and quantification were performed by the NovoGene Database of NovoGene Co., Ltd. (Beijing, China). Tissues (100 mg) were individually ground with liquid nitrogen, and the homogenate was re-suspended with pre-chilled 80% methanol and 0.1% formic acid by vortexing. The supernatant was injected into an LC-MS/MS system. UHPLC-MS/MS analyses were performed using a Vanquish UHPLC system (ThermoFisher, Dreieich, Germany) coupled with an Orbitrap Q Exactive™ HF mass spectrometer (ThermoFisher). Structural analysis of metabolites was determined using standard metabolic operating procedures. MRM was used to conduct metabolite quantification. All metabolites identified were subject to partial least squares discriminant analysis. Principle component analysis (PCA) and Orthogonal Partial Least Squares Discriminate Analysis (OPLS-DA) were carried out to identify potential biomarker variables. For potential biomarker selection, variable importance in projection (VIP)  $\geq 1$  and fold change (FC)  $\geq 2$  or  $\leq 0.5$  were set for metabolites with significant differences.

#### 4.5. Yeast Two-Hybrid Assay

The amplified full-length CDSs of *SIPIF1*, *SIPIF3*, *SIAN2-like*, *SIAN2*, *SIAN11*, *SIAN1*, *SIHY5*, *SIJAF13*, *SIBBX24* and *SIWRKY44* were amplified and inserted into pGADT7 and pGBKT7 vectors, respectively. Primers used for amplified and plasmid construction are listed in Supplementary Table S1. Different combinations of bait and prey vectors were co-transformed into Y2Hgold and then cultured on SD/-Leu-Trp (SD-LT) medium supplemented at 28 °C for 2–3 days. Next, 2.5 µL of aliquots were patched on SD/Ade/His/Leu/Trp plates with 5-bromo-4-chloro-3-indolyl- $\alpha$ -D-galactopyranoside (X- $\alpha$ -Gal) and incubated at 28 °C for 3 days.

#### 4.6. Virus-Induced *SIBBX24* Gene Silencing in Tomato

Specific coding regions *SIBBX24* fragment were selected for VIGS vector construction by the VIGS design tool (<http://solgenomics.net/tools/vigs>, accessed on 10 November 2022). A 300 bp fragment of the coding region of *SIBBX24* was amplified using the forward primer (5'-gtgagtaagggtaccgaattc ATGAAGATACAGTGTGATGTG-3') and the reverse primer (5'-cgtgagctcggtagccgatcc AGTGGCTAAGAAGCGTTGGTG-3'). The PCR product was ligated into the *pTRV2* vector to construct the *TRV2::SIBBX24* vector. The recombinant plasmid and *TRV1* vector were transferred into *Agrobacterium* GV3101. Resuspensions of *pTRV1* and *pTRV2* (as a negative control) or its derivative vectors were mixed at a 1:1 ratio and then infiltrated into a mature green-stage tomato. The injected fruits were grown in a growth chamber at 22 ± 2 °C, and 12 h of light/12 h of darkness, and relative humidity was controlled in the range of 70 ± 5%. After two weeks, fruits were harvested and stored at −80 °C for RNA and qRT-PCR analysis to assess the degree of silencing.

#### 4.7. Luciferase Complementation Imaging Assays (LCI)

The full-length CDS of *SIBBX24* was amplified and cloned, and ligated into *pCAMBIA1300-35S-cLUC* to produce *SIBBX24-nLUC*. *SIHY5*, *SIPIF1*, *SIPIF3*, *SIAN2-like*, *SIAN2*, *SIAN11* were fused with *pCAMBIA1300-35S-cLUC* to generate the *cLUC-SIHY5*, *cLUC-SIPIF1*, *cLUC-SIPIF3*, *cLUC-SIAN2-like*, *cLUC-SIAN2* and *cLUC-SIAN11*. *Agrobacterium* strains GV3101 containing the above constructs were infiltrated into the leaves of 6-week-old *N. benthamiana* plants. The leaf images were captured after a 1 d incubation in darkness at 22 °C and an additional 1 d incubation under a 16-h light/8-h dark photoperiod.

#### 4.8. RNA Extraction and Quantitative Reverse Transcription PCR

Total RNA was extracted from different parts of the seedling and the peel of fruit using RNAex Pro Reagent (Accurate Biotechnology Co., Ltd., Changsha, China), and its quality and quantity were evaluated using a Nanodrop ND-1000 spectrophotometer (Thermo Fisher Scientific, Waltham, MA, USA). The first cDNA strand was synthesized using Evo M-MLV RT for PCR Kit (Accurate Biotechnology Co., Ltd., Changsha, China). The relative expression levels were determined by performing a quantitative reverse transcription PCR (qRT-PCR) analysis using a LightCycler 480 system (Roche, Hercules, Switzerland) with an Evo M-MLV RT-PCR kit (Accurate Biotechnology Co., Ltd., Changsha, China). The PCR thermocycling protocol was as follows: 95 °C for 30 s, followed by 40 cycles of 95 °C for 15 s and annealing for 60 °C for 30 s. Three biological replicates and three qRT-PCR technical replicates were performed for each sample. The relative expression levels were normalized with the results of mean values of *SIUBI* using the  $2^{-\Delta\Delta C_t}$  method [54]. The primer sequences used for the qRT-PCR analyses are listed in Table S1.

#### 4.9. Statistical Analysis

All values are shown as the means of three replicates with standard error (SE). Analysis of variance was performed by Duncan's multiple range test using the SPSS 22.0 program (SPSS 22.0, SPSS Inc., Chicago, IL, USA). Different significance of means was tested by LSD at  $p < 0.05$ . Graphs were plotted using Origin 2021 (Origin Lab Corporation, Northampton, MA, USA). The heat map analysis was visualized by TBtools software (TBtools-II v1.120) [55].

## 5. Conclusions

HY5 has a pivotal role in regulating anthocyanin accumulation in tomatoes. *Sllhy5* mutants were created via the CRISPR/Cas9 system from 'Indigo Rose'. *Sllhy5* mutants displayed significantly lower anthocyanin accumulation than InR, both in seedlings and fruit. Interestingly, detectable levels of anthocyanins were present in *hy5* mutant seedlings and fruit, and the pigment accumulation displayed obvious spatiotemporal specificity in the *Sllhy5* seedling. These results indicated that other regulators existed to regulate anthocyanin biosynthesis in an HY5-independent manner. The total amount of flavonoids in InR was significantly higher

than in the *Sllhy5* mutant, and most of the genes associated with anthocyanin biosynthesis displayed higher expression levels in InR. *SIBBX24* likely regulated anthocyanin biosynthesis by interacting with *SIAN2-like*, *SIAN2*, while *SIWRKY44* interacted with *SIAN11*. Moreover, *SIPIF1* and *SIPIF3* seemed to be involved in anthocyanin biosynthesis by interacting with *SIBBX24*. We identified *SIBBX24* as a target to silence to produce fewer anthocyanins in tomato fruit peel, indicating the important role of *SIBBX24* in the regulation of anthocyanin accumulation. These results deepened the understanding of purple color formation in tomato seedlings and fruits in an *HY5*-dependent or independent manner via excavating the genes involved in anthocyanin biosynthesis. This study will help with the functional analysis of candidate genes controlling the color components of tomatoes and provide a theoretical basis for the breeding of tomatoes with high anthocyanin accumulation.

**Supplementary Materials:** The following supporting information can be downloaded at: <https://www.mdpi.com/article/10.3390/ijms24108690/s1>.

**Author Contributions:** R.H. and H.L. designed the project. R.H., K.L., J.J., Y.H. and S.Z. performed experiments. R.H., H.L., Y.L. and X.L. analyzed the data. R.H., K.L. and H.L. wrote the article. All authors have read and agreed to the published version of the manuscript.

**Funding:** This work was supported by a grant from the Key-Area Research and Development Program of Guangdong Province (2019B020214005 and 2019B020222003).

**Institutional Review Board Statement:** Animals. Not applicable.

**Informed Consent Statement:** Not applicable.

**Data Availability Statement:** Not applicable.

**Conflicts of Interest:** The authors declare that they have no known competing financial interests or personal relationships that could have appeared to influence the work reported in this paper.

## References

1. Tsuda, T. Dietary anthocyanin-rich plants: Biochemical basis and recent progress in health benefits studies. *Mol. Nutr. Food Res.* **2012**, *56*, 159–170. [[CrossRef](#)] [[PubMed](#)]
2. Koes, R.; Verweij, W.; Quattrocchio, F. Flavonoids: A colorful model for the regulation and evolution of biochemical pathways. *Trends Plant Sci.* **2005**, *10*, 236–242. [[CrossRef](#)] [[PubMed](#)]
3. Rossi, A.; Serraino, I.; Dugo, P.; Paola, R.D.; Mondello, L.; Genovese, T.; Morabito, D.; Dugo, G.; Sautebin, L.; Caputi, A.P.; et al. Protective effects of anthocyanins from blackberry in a rat model of acute lung inflammation. *Free Radic. Res.* **2003**, *37*, 891–900. [[CrossRef](#)]
4. Gonzali, S.; Perata, P. Anthocyanins from purple tomatoes as novel antioxidants to promote human health. *Antioxidants* **2020**, *9*, 1017. [[CrossRef](#)] [[PubMed](#)]
5. Outchkourov, N.S.; Karlova, R.; Hölscher, M.; Schrama, X.; Blilou, I.; Beekwilder, J. Transcription factor-mediated control of anthocyanin biosynthesis in vegetative tissues 1. *Plant Physiol.* **2018**, *176*, 1862–1878. [[CrossRef](#)] [[PubMed](#)]
6. Butelli, E.; Bulling, K.; Hill, L.; Martin, C. Beyond purple tomatoes: Combined strategies targeting anthocyanins to generate crimson, magenta, and indigo fruit. *Horticulturae* **2021**, *7*, 327. [[CrossRef](#)]
7. Petroni, K.; Tonelli, C. Recent advances on the regulation of anthocyanin synthesis in reproductive organs. *Plant Sci.* **2011**, *181*, 219–229. [[CrossRef](#)]
8. Boase, M.R.; Ngo, H.; Jameson, P.E.; Schwinn, K.E. A conserved network of transcriptional activators and repressors regulates anthocyanin pigmentation in Eudicots. *Plant Cell* **2014**, *26*, 962–980. [[CrossRef](#)]
9. Lloyd, A.; Brockman, A.; Aguirre, L.; Campbell, A.; Bean, A.; Cantero, A.; Gonzalez, A. Advances in the MYB-bHLH-WD Repeat (MBW) pigment regulatory model: Addition of a WRKY factor and co-option of an anthocyanin MYB for betalain regulation. *Plant Cell Physiol.* **2017**, *58*, 1431–1441. [[CrossRef](#)]
10. Bursch, K.; Niemann, E.T.; Nelson, D.C.; Johansson, H. KARRIKINS control seedling photomorphogenesis and anthocyanin biosynthesis through a HY5-BBX transcriptional module. *Plant J.* **2021**, *107*, 1346–1362. [[CrossRef](#)]
11. Qiu, Z.; Wang, H.; Li, D.; Yu, B.; Hui, Q.; Yan, S.; Huang, Z.; Cui, X.; Cao, B. Identification of candidate HY5-dependent and -independent regulators of anthocyanin biosynthesis in tomato. *Plant Cell Physiol.* **2019**, *60*, 643–656. [[CrossRef](#)] [[PubMed](#)]
12. Xiong, C.; Luo, D.; Lin, A.; Zhang, C.; Shan, L.; He, P.; Li, B.; Zhang, Q.; Hua, B.; Yuan, Z.; et al. A tomato B-box protein *SIBBX20* modulates carotenoid biosynthesis by directly activating PHYTOENE SYNTHASE 1, and is targeted for 26S proteasome-mediated degradation. *N. Phytol.* **2019**, *221*, 279–294. [[CrossRef](#)] [[PubMed](#)]
13. Datta, S.; Hettiarachchi, C.; Johansson, H.; Holm, M. Salt tolerance homolog 2, a B-box protein in Arabidopsis that activates transcription and positively regulates light-mediated development. *Plant Cell* **2007**, *19*, 3242–3255. [[CrossRef](#)]

14. Datta, S.; Johansson, H.; Hettiarachchi, C.; Irigoyen, M.L.; Desai, M.; Rubio, V.; Holm, M. LZFI/SALT TOLERANCE HOMOLOG3, an Arabidopsis B-box protein involved in light-dependent development and gene expression, undergoes COP1-mediated ubiquitination. *Plant Cell* **2008**, *20*, 2324–2338. [[CrossRef](#)] [[PubMed](#)]
15. Yadav, A.; Ravindran, N.; Singh, D.; Rahul, P.V.; Datta, S. Role of Arabidopsis BBX proteins in light signaling. *J. Plant Biochem. Biotechnol.* **2020**, *29*, 623–635. [[CrossRef](#)]
16. Zhang, X.; Huai, J.; Shang, F.; Xu, G.; Tang, W.; Jing, Y.; Lin, R. A PIF1/PIF3-HY5-BBX23 transcription factor cascade affects photomorphogenesis. *Plant Physiol.* **2017**, *174*, 2487–2500. [[CrossRef](#)]
17. Gangappa, S.N.; Crocco, C.D.; Johansson, H.; Datta, S.; Hettiarachchi, C.; Holm, M.; Botto, J.F. The Arabidopsis B-BOX protein BBX25 interacts with HY5, negatively regulating *BBX22* expression to suppress seedling photomorphogenesis. *Plant Cell* **2013**, *25*, 1243–1257. [[CrossRef](#)]
18. Job, N.; Yadukrishnan, P.; Bursch, K.; Datta, S.; Johansson, H. Two B-box proteins regulate photomorphogenesis by oppositely modulating HY5 through their diverse C-terminal domains. *Plant Physiol.* **2018**, *176*, 2963–2976. [[CrossRef](#)]
19. Holtan, H.E.; Bandong, S.; Marion, C.M.; Adam, L.; Tiwari, S.; Shen, Y.; Maloof, J.N.; Maszle, D.R.; Ohto, M.-A.; Preuss, S.; et al. BBX32, an arabidopsis b-box protein, functions in light signaling by suppressing HY5-regulated gene expression and interacting with *STH2/BBX21*. *Plant Physiol.* **2011**, *156*, 2109–2123. [[CrossRef](#)]
20. Luo, D.; Xiong, C.; Lin, A.; Zhang, C.; Sun, W.; Zhang, J.; Yang, C.; Lu, Y.; Li, H.; Ye, Z.; et al. *SIBBX20* interacts with the COP9 signalosome subunit *SICSN5-2* to regulate anthocyanin biosynthesis by activating *SIDFR* expression in tomato. *Hortic. Res.* **2021**, *8*, 163. [[CrossRef](#)]
21. Zhang, B.; Yang, H.J.; Qu, D.; Zhu, Z.Z.; Yang, Y.Z.; Zhao, Z.Y. The MdBBX22–miR858–MdMYB9/11/12 module regulates proanthocyanidin biosynthesis in apple peel. *Plant Biotechnol. J.* **2022**, *20*, 1683–1700. [[CrossRef](#)] [[PubMed](#)]
22. Shin, D.H.; Choi, M.; Kim, K.; Bang, G.; Cho, M.; Choi, S.B.; Choi, G.; Park, Y.I. HY5 regulates anthocyanin biosynthesis by inducing the transcriptional activation of the MYB75/PAP1 transcription factor in Arabidopsis. *FEBS Lett.* **2013**, *587*, 1543–1547. [[CrossRef](#)] [[PubMed](#)]
23. Verweij, W.; Spelt, C.E.; Bliet, M.; de Vries, M.; Wit, N.; Faraco, M.; Koes, R.; Quattrocchio, F.M. Functionally similar WRKY proteins regulate vacuolar acidification in petunia and hair development in arabidopsis. *Plant Cell* **2016**, *28*, 786–803. [[CrossRef](#)] [[PubMed](#)]
24. Alabd, A.; Ahmad, M.; Zhang, X.; Gao, Y.; Peng, L.; Zhang, L.; Ni, J.; Bai, S.; Teng, Y. Light-responsive transcription factor PpWRKY44 induces anthocyanin accumulation by regulating PpMYB10 expression in pear. *Hortic. Res.* **2022**, *9*, 199. [[CrossRef](#)]
25. Mes, P.J.; Boches, P.; Myers, J.R.; Durst, R. Characterization of tomatoes expressing anthocyanin in the fruit. *J. Am. Soc. Hortic. Sci.* **2008**, *133*, 262–269. [[CrossRef](#)]
26. Vu, A.T.; Lee, J.M. Genetic variations underlying anthocyanin accumulation in tomato fruits. *Euphytica* **2019**, *215*, 196. [[CrossRef](#)]
27. Sun, C.; Deng, L.; Du, M.; Zhao, J.; Chen, Q.; Huang, T.; Jiang, H.; Li, C.B.; Li, C. A transcriptional network promotes anthocyanin biosynthesis in tomato flesh. *Mol. Plant* **2019**, *13*, 42–58. [[CrossRef](#)]
28. Ha, H.T.N.; Van Tai, N.; Thuy, N.M. Physicochemical characteristics and bioactive compounds of new black cherry tomato (*Solanum lycopersicum*) varieties grown in Vietnam. *Plants* **2021**, *10*, 2134. [[CrossRef](#)]
29. Gangappa, S.N.; Botto, J.F. The Multifaceted roles of HY5 in plant growth and development. *Mol. Plant* **2016**, *9*, 1353–1365. [[CrossRef](#)]
30. Shin, J.; Park, E.; Choi, G. PIF3 regulates anthocyanin biosynthesis in an HY5-dependent manner with both factors directly binding anthocyanin biosynthetic gene promoters in Arabidopsis. *Plant J.* **2007**, *49*, 981–994. [[CrossRef](#)]
31. Chen, R.; Yang, C.; Gao, H.; Shi, C.; Zhang, Z.; Lu, G.; Shen, X.; Tang, Y.; Li, F.; Lu, Y.; et al. Induced mutation in *ELONGATED HYPOCOTYL5* abolishes anthocyanin accumulation in the hypocotyl of pepper. *Theor. Appl. Genet.* **2022**, *135*, 3455–3468. [[CrossRef](#)] [[PubMed](#)]
32. Lee, J.; He, K.; Stolc, V.; Lee, H.; Figueroa, P.; Gao, Y.; Tongprasit, W.; Zhao, H.; Lee, I.; Xing, W.D. Analysis of transcription factor HY5 genomic binding sites revealed its hierarchical role in light regulation of development. *Plant Cell* **2007**, *19*, 731–749. [[CrossRef](#)] [[PubMed](#)]
33. Mohammadi-Shemirani, P.; Sood, T.; Paré, G. From ‘Omics to multi-omics technologies: The discovery of novel causal mediators. *Curr. Atheroscler. Rep.* **2023**, *25*, 55–65. [[CrossRef](#)] [[PubMed](#)]
34. Tiedge, K.; Li, X.; Merrill, A.T.; Davison, D.; Chen, Y.; Yu, P.; Tantillo, D.J.; Last, R.L.; Zerbe, P. Comparative transcriptomics and metabolomics reveal specialized metabolite drought stress responses in switchgrass (*Panicum virgatum*). *N. Phytol.* **2022**, *236*, 1393–1408. [[CrossRef](#)]
35. Rothenberg, D.O.N.; Yang, H.; Chen, M.; Zhang, W.; Zhang, L. Metabolome and transcriptome sequencing analysis reveals anthocyanin metabolism in pink flowers of anthocyanin-rich tea (*Camellia sinensis*). *Molecules* **2019**, *24*, 1064. [[CrossRef](#)]
36. Datir, S.; Regan, S. Advances in physiological, transcriptomic, proteomic, metabolomic, and molecular genetic approaches for enhancing Mango fruit quality. *J. Agric. Food Chem.* **2022**, *71*, 20–34. [[CrossRef](#)]
37. Roumani, M.; Le Bot, J.; Boisbrun, M.; Magot, F.; Péré, A.; Robin, C.; Hilliou, F.; Larbat, R. Transcriptomics and metabolomics analyses reveal high induction of the phenolamide pathway in tomato plants attacked by the *Leafminer Tuta absoluta*. *Metabolites* **2022**, *12*, 484. [[CrossRef](#)]
38. Wang, Z.R.; Cui, Y.Y.; Vainstein, A.; Chen, S.W.; Ma, H.Q. Regulation of fig (*Ficus carica* L.) fruit color: Metabolomic and transcriptomic analyses of the flavonoid biosynthetic pathway. *Front. Plant. Sci.* **2017**, *8*, 1990. [[CrossRef](#)]

39. Roldan, M.V.G.; Engel, B.; de Vos, R.C.H.; Vereijken, P.; Astola, L.; Groenenboom, M.; van de Geest, H.; Bovy, A.; Molenaar, J.; van Eeuwijk, F.; et al. Metabolomics reveals organ-specific metabolic rearrangements during early tomato seedling development. *Metabolomics* **2014**, *10*, 958–974. [[CrossRef](#)]
40. Li, Y.; Chen, Y.; Zhou, L.; You, S.; Deng, H.; Chen, Y.; Alseekh, S.; Yuan, Y.; Fu, R.; Zhang, Z.; et al. MicroTom metabolic network: Rewiring tomato metabolic regulatory network throughout the growth cycle. *Mol. Plant* **2020**, *13*, 1203–1218. [[CrossRef](#)]
41. Colanero, S.; Tagliani, A.; Perata, P.; Gonzali, S. Alternative splicing in the anthocyanin fruit gene encoding an R2R3 MYB transcription factor affects anthocyanin biosynthesis in tomato fruits. *Plant Commun.* **2020**, *1*, 100006. [[CrossRef](#)] [[PubMed](#)]
42. Naing, A.H.; Kim, C.K. Roles of R2R3-MYB transcription factors in transcriptional regulation of anthocyanin biosynthesis in horticultural plants. *Plant Mol. Biol.* **2018**, *98*, 1–18. [[CrossRef](#)] [[PubMed](#)]
43. Schreiber, G.; Reuveni, M.; Evenor, D. Anthocyanin1 from *Solanum chilense* is more efficient in accumulating anthocyanin metabolites than its *Solanum lycopersicum* counterpart in association with the anthocyanin fruit phenotype of tomato. *Theor. Appl. Genet.* **2012**, *124*, 295–307. [[CrossRef](#)]
44. Kiferle, C.; Fantini, E.; Bassolino, L.; Povero, G.; Spelt, C.; Perata, P.; Gonzali, S. Tomato R2R3-MYB proteins SIANT1 and SIAN2: Same protein activity, different roles. *PLoS ONE* **2015**, *10*, e0136365. [[CrossRef](#)] [[PubMed](#)]
45. Meng, X.; Yang, D.; Li, X.; Zhao, S.; Sui, N.; Meng, Q. Physiological changes in fruit ripening caused by overexpression of tomato SIAN2, an R2R3-MYB factor. *Plant Physiol. Biochem.* **2015**, *89*, 24–30. [[CrossRef](#)] [[PubMed](#)]
46. Subban, P.; Prakash, S.; Mann, A.B.; Kutsher, Y.; Evenor, D.; Levin, I.; Reuveni, M. Functional analysis of MYB alleles from *Solanum chilense* and *Solanum lycopersicum* in controlling anthocyanin levels in heterologous tobacco plants. *Physiol. Plant.* **2021**, *172*, 1630–1640. [[CrossRef](#)]
47. Gao, Y.; Liu, J.; Chen, Y.; Tang, H.; Wang, Y.; He, Y.; Ou, Y.; Sun, X.; Wang, S.; Yao, Y. Tomato SIAN11 regulates flavonoid biosynthesis and seed dormancy by interaction with bHLH proteins but not with MYB proteins. *Hortic. Res.* **2018**, *5*, 27. [[CrossRef](#)]
48. Stracke, R.; Favory, J.J.; Gruber, H.; Bartelniewoehner, L.; Bartels, S.; Binkert, M.; Funk, M.; Weisshaar, B.; Ulm, R. The Arabidopsis bZIP transcription factor HY5 regulates expression of the *PFG1/MYB12* gene in response to light and ultraviolet-B radiation. *Plant Cell Environ.* **2010**, *33*, 88–103. [[CrossRef](#)]
49. Wang, Y.; Zhang, X.; Zhao, Y.; Yang, J.; He, Y.; Li, G.; Ma, W.; Huang, X.; Su, J. Transcription factor *PyHY5* binds to the promoters of *PyWD40* and *PyMYB10* and regulates its expression in red pear ‘Yunhongli No. 1’. *Plant Physiol. Biochem.* **2020**, *154*, 665–674. [[CrossRef](#)]
50. Zhi, J.; Liu, X.; Li, D.; Huang, Y.; Yan, S.; Cao, B.; Qiu, Z. CRISPR/Cas9-mediated *SIAN2* mutants reveal various regulatory models of anthocyanin biosynthesis in tomato plant. *Plant Cell Rep.* **2020**, *39*, 799–809. [[CrossRef](#)] [[PubMed](#)]
51. Quattrocchio, F.; Verweij, W.; Kroon, A.; Spelt, C.; Mol, J.; Koes, R. PH4 of petunia is an R2R3 MYB protein that activates vacuolar acidification through interactions with basic-helix-loop-helix transcription factors of the anthocyanin pathway. *Plant Cell* **2006**, *18*, 1274–1291. [[CrossRef](#)] [[PubMed](#)]
52. Qin, J.; Zhao, C.; Wang, S.; Gao, N.; Wang, X.; Na, X.; Wang, X.; Bi, Y. PIF4-PAP1 interaction affects MYB-bHLH-WD40 complex formation and anthocyanin accumulation in Arabidopsis. *J. Plant Physiol.* **2022**, *268*, 153558. [[CrossRef](#)] [[PubMed](#)]
53. Rapisarda, P.; Fanella, F.; Maccarone, E. Reliability of analytical methods for determining anthocyanins in blood orange juices. *J. Agric. Food Chem.* **2000**, *48*, 2249–2252. [[CrossRef](#)] [[PubMed](#)]
54. Livak, K.J.; Schmittgen, T.D. Analysis of relative gene expression data using real-time quantitative PCR and the  $2^{-\Delta\Delta CT}$  method. *Methods* **2001**, *25*, 402–408. [[CrossRef](#)] [[PubMed](#)]
55. Chen, C.; Chen, H.; Zhang, Y.; Thomas, H.R.; Frank, M.H.; He, Y.; Xia, R. TBtools: An integrative toolkit developed for interactive analyses of big biological data. *Mol. Plant* **2020**, *13*, 1194–1202. [[CrossRef](#)]

**Disclaimer/Publisher’s Note:** The statements, opinions and data contained in all publications are solely those of the individual author(s) and contributor(s) and not of MDPI and/or the editor(s). MDPI and/or the editor(s) disclaim responsibility for any injury to people or property resulting from any ideas, methods, instructions or products referred to in the content.